Virchows Arch A (1987) 411:425–434

Virchows Archiv A

Sequestration hypothesis of atherosclerosis

Richard E. Tracy [1], Grace E. Kissling [2], Gray T. Malcom [1], and Kenneth Devaney [3]

[1] LSUMC, Department of Pathology, 1901 Perdido Street, New Orleans, LA 70112-1393, USA
[2] Department of Mathematics, University of North Carolina at Greensboro, Greensboro, NC 27412, USA
[3] Naval Health Science Education and Training Command, Naval Medical Command, National Capital Region, Bethesda, Maryland, USA

Summary. Atherosclerosis of the human aorta has been studied by morphometric, chemical, and histochemical methods. Results of these separate approaches are converging upon a theory of pathogenesis. This theory begins with the standard view of a two stage process, intimal fibroplasia followed by atheronecrosis in the most thickened and aged places. The first stage, fibroplasia, can be described in terms of a stochastic process wherein smooth muscle cells, scattered in accordance with a Poisson distribution, elaborate matrix materials over time, causing the realms of the cells to expand and to aggregate. The fusion of the expanded smooth muscle cell realms seems to mark the advent of necrosis. The second stage, atheronecrosis, can be described such that the probability of a necrotic core emerging at a site in a vessel is governed by the amount and the age of interstitial matrix materials at the site. Further evidence shows that the matrix materials tend to sequester lipids in greater than proportionate amounts as the intimal bulk increases. The sequestered perifibrous lipid is histochemically different from the lipids of the necrotic core, in that only the latter can be fixed with chromic acid. These results suggest that lipids undergo a qualitative change as well as a quantitative increase at the stage of impending necrosis. This qualitative change is governed by age, which raises the possibility that necrotizing toxicity accumulates in the sequestered lipid as it ages.

Key words: Atherosclerosis – Sequestration hypothesis – Human aorta

Introduction

The necrotic core which characterizes advanced atherosclerotic lesions is thought to be preceded by fibrotic intimal thickenings (Benditt 1977). In the terminology used by Scott et al. (1967) for the human and applied by Kritchevsky et al. (1976) and Wissler (1974) to primates and rabbits, the process begins with a proliferative phase that is followed by an atheromatous phase. Velican and Velican (1985) have provided extensive data to document this pathogenetic sequence. By measuring the fibroproliferative tissue in the cap and base of necrotic lesions in human aorta, the concept of a threshold was proposed (Tracy et al. 1979b). Intima of approximately 300 to 400 μm thickness was found to have an appreciable probability of containing a necrotic core, and this probability rose with further thickening. Later data suggested that the threshold was high in youth and declined with age (Tracy et al. 1985b; 1987a). These findings raise two especially interesting questions. Why should fibrotically thickened intima be at risk of a necrotic transformation, and why should this risk increase as the fibrotic tissue ages?

Data provided by Malcom et al. (1984) indicate that the intima of the human aorta has the capacity to store cholesterol, cholesterol ester, and phospholipid, and that this capacity increases as the bulk of intimal tissue grows. This is also true of blood lipoproteins (Smith and Ashall 1984). Aging of the lipid in human aorta is associated with the accumulation of toxic materials (VanLier and Smith 1967; Taylor et al. 1979; Jachau 1979; Ferrario et al. 1985). These considerations lead to the proposal that the aging of sequestered liquid could produce threshold amounts of toxic materials. Thereafter, atheronecrosis might intervene as foam cells take in the toxic materials, die, then add their substances to the plaque's necrotic core (Chait 1983; Stary 1984).

The hypothesis that sequestered lipid becomes toxic generates some predictions about the behavior of certain measurable properties of the artery wall. Those predictions are open to observational testing. Several tests of this kind comprise the main

Offprint requests to: R.E. Tracy

body of this communication. Some details about how the preatheromatous fibroplasia evolves in preparation for the necrotic transformation are considered in the appendix.

Materials and methods

Selection of cases. Three independent series of cases, compiled in different ways, provided data for use in this inquiry. Details about these three series are given elsewhere (Tracy et al. 1983a; Tracy et al. 1986; Malcom et al. 1984); they will be only briefly described here. a) 8-populations study: Aortas from men and women aged 15–69 autopsied in Bogota, Durban (Bantu and Indian), Manila, Mexico, New Orleans (Negro and White), and Sao Paulo, Brazil were retrieved from the Archive of the International Atherosclerosis Project where they have been stored in plastic bags. About 1/3 of the arteries were later found to be excessively dry from storage and could not be prepared for microscopy, leaving a total of 686 completed cases. b) CHD study: A series of cases aged 30–64 in which coronary heart disease was the cause of death were assembled from a coroner's service. Each case was matched with one or more age-sex-race equivalent subject who had no evidence of cardiovascular disease at autopsy. c) G-NO study: Aortas were obtained at autopsy in New Orleans (white only) and Guatemala City from 15 men in each of the age groups 15 to 24, 25 to 34, 35 to 44, and 45 to 54, without regard to cause of death.

Morphometry of thoracic aortas. For the CHD and 8-populations studies, samples were excised from the lateral thoracic aortas, decalcified and blocked in paraffin. H&E-stained 11 μm sections were marked at 20 equally spaced positions from the 4th to the 12th intercostal ostia along the left and right samples, 40 points in all. Atheronecrosis is operationally defined as a region of necrotic core with cholesterol clefts easily discerned under 40X objective lens. The proportion of sample seen to be affected by atheronecrosis, P_A, was recorded. Intimal thicknesses measured with an eyepiece ruler at the 40-N nonnecrotic points were averaged to yield the mean nonnecrotic intimal thickness, F. Interobserver correlations for F and P_A were 0.996 and 0.938 in a previous report that examines these methods in details (Tracy et al. 1983a, b). The density of smooth muscle cells, used in the appendix for the computation of the realm, was obtained by enumeration of nuclear profiles. The details of this procedure are given elsewhere (Tracy et al. 1987b). Briefly, a band of 100 μm width extending F micrometers from the luminal surface to the intima-media boundary is examined under the 40X lens. The hematoxylin-stained nuclear profiles are counted and their number is C_T. Cell density is $C_D = C_T/F$, where F is measured in 100 μm units.

Chemical analyses. For the G-NO study, the left half of the abdominal aorta was formalin-fixed and sectioned at 12 sites for histologic examination. Based on these 12 sites, each aorta was classified either as having or as not having at least one instance of atheronecrosis. From the right half of the specimen, the intima was dissected, dried, weighed, and extracted with lipid solvents. The total lipid, L, was determined gravimetrically. The dry defatted weight, W, was determined by subtraction of milligrams of total lipid in each sample from milligrams of dry tissue. These measurements are expressed as milligrams per square centimeter of aortic area. Aliquots of the lipid extract were used to quantify cholesterol ester, free cholesterol and phospholipid by methods previously described (Malcom et al. 1984), and each was expressed as mg/cm^2.

Chromate fixation. Using a suggestion by Wiggleworth (1981) we modified our former method for chromate fixation of lipids as follows. Solution A: 3 ml myrcene (Aldrich, tech,) + 200 ml 60% isopropanol. Solution B: 50 ml 5% chromium tetroxide + 200 ml 80% ethanol, use in freezer at −19 °C, make fresh for each use. Bits of formalin-fixed tissues are twice passed sequentially through Solution A – 3 days; Solution B – 24 hours; water – 3 days. These tissue samples are then processed into paraffin as usual, sectioned at 11 μm and stained with Oil red O – hematoxylin. Aortic samples were split into frozen sections and chromated paraffin sections in such a way that facing surfaces were sectioned to be as close together as possible.

Results

Intimal bulk and lipid content

As the intimal bulk measured by dry defatted weight (W) increases, each unit of tissue manifests an increasing ability to retain lipid. This result is seen graphically in Fig. 1; it can also be shown by regression analysis. Suppose that the lipid content, L, is a fixed proportion of the dry tissue ($L+W$), i.e., $p = L/(L+W)$. If this is true, it can be shown that the relationship, $\log L = \beta \log W + \delta$ requires $\beta = 1$. The direct proportionality between L and $L+W$ would then be represented by a linear relationship between $\log L$ and $\log W$. The observed linear regression equation for the 154 cases has $\beta = 1.447 \pm$ a standard error of 0.0638, thus rejecting $\beta = 1$ ($R^2 = 0.772$). Since the observed estimate of β is greater than 1, the proportion of lipid increases with intimal bulk. In Fig. 1, a line representing $p = 1:6$ is introduced to illustrate the obvious poor fit obtained by choosing p to be a con-

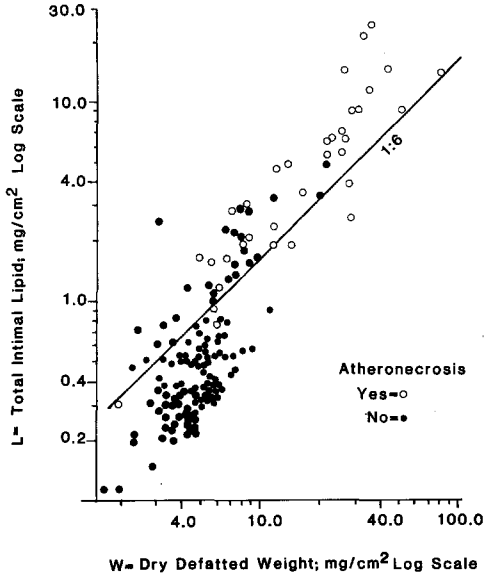

Fig. 1. A line representing a constant ratio of 1:6 is introduced to aid discussion. Any line of constant ratio between L and W must be parallel to this one of 1:6

Table 1. Correlation coefficients among lipid measures and dry defatted weight after logarithmic transformation; 154 half abdominal aortas, ages 15–54

		TC	PL	CE	FC	W	AGE
Total Lipid	TL	0.985	0.969	0.947	0.977	0.879	0.624
Total Cholesterol	TC	–	0.945	0.964	0.981	0.849	0.626
Phospholipid	PL	–	–	0.888	0.971	0.913	0.598
Cholesterolester	CE	–	–	–	0.898	0.782	0.604
Free Cholesterol	FC	–	–	–	–	0.897	0.628
Dry Defatted Weight	W	–	–	–	–	–	0.483

stant and $\beta = 1$. Other lines of constant ratio different from 1:6 would be parallel to this one and also clearly unsuitable.

At each magnitude of intimal bulk, the ability to retain lipid increases with age. The linear regression equation, $\log L = 1.131 \log (\text{Age} \times W) - 6.246$ ($R^2 = 0.818$) expresses this finding. The broken lines in Fig. 2 illustrate this relationship for three values of L chosen from a wide range.

Individual classes of lipid also related in a linear way to each other and to W on log-log plots (Table 1). Regression equations are reported here for general interest: log (cholesterol ester) = 1.582 log $W - 4.833$ ($R^2 = 0.611$), log (free cholesterol) = 1.763 log $W - 5.525$ ($R^2 = 0.805$); log (phospholipid) = 1.288 log $W - 3.990$ ($R^2 = 0.833$).

Intimal bulk and atheronecrosis

The probability of finding atheronecrosis in an aorta increases with intimal bulk and with age. This result is seen graphically in Fig. 2. Aortas in which at least one instance of necrotic core were found, represented by open circles, were those with greater dry defatted weights of dissected intimal tissue and greater ages. The finding can be described by a discriminant function, $D = 3.811 \log (\text{Age} \times W) - 21.98$ ($R^2 = 0.521$). The solid curve in Fig. 2 represents this equation with $D = 0$ marking the threshold between no necrotic cores and one or more necrotic cores. If D is greater than 0, meaning that a point is above the line in Fig. 2, then the aorta is more likely than not to have a necrotic core in the observed sample. Notice that the threshold amount of intimal tissue accompanying the onset of atheronecrosis declines with age from roughly 9.14 mg/cm^2 at age 35 to about 5.83 at age 55, a decline of 36%.

Intimal thickness and atheronecrosis

The probability of finding atheronecrosis can also be shown to increase with intimal bulk by measuring the bulk in histologic sections in the form of intimal thickness at the nonnecrotic positions (F). In Fig. 3, aortas with at least one instance of necrotic core, represented by open circles, tend to be those with greater nonnecrotic intimal thicknesses, and greater ages. The result can also be shown by a discriminant function, $D = 0.000255$ Age (F-77) $- 3.06$ ($R^2 = 0.444$). Again, the threshold declines with age from about 420 μm at age 35 to 295 at age 55, a decline of 30%.

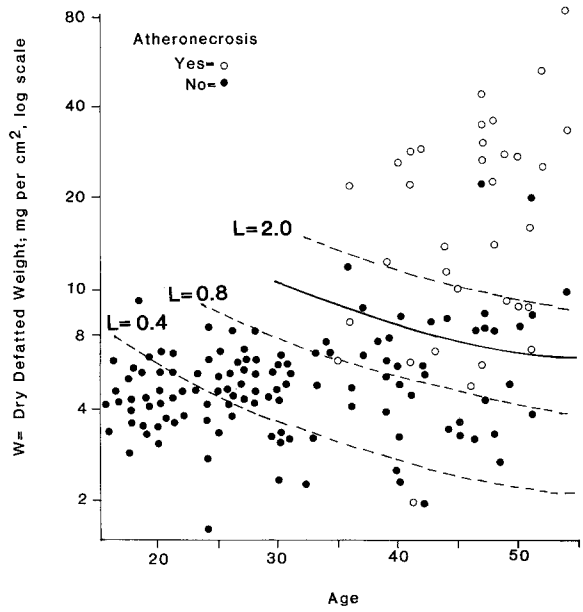

Fig. 2. Discriminant function (*solid curve*) and regression equations reflecting selected values of L (*dashed curves*) are superimposed on the data for 154 cases of the G-NO study

This result can also be shown with regression analysis. The percentage of the specimen affected by necrotic cores, P_A, is best predicted by $\sqrt{P_A} = 0.000162$ Age (F-170) $+ 0.26$ ($R^2 = 0.565$). The probability of finding a necrotic core in a randomly chosen point in the sample, P_A, can be found from this equation, which is plotted in Fig. 3 as dashed curves.

An independent series of 145 cases, the CHD study (see methods), gave similar results. $D =$

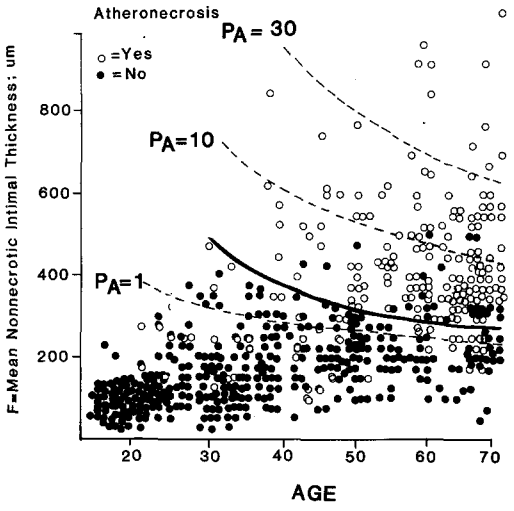

Fig. 3. Discriminant function (*solid curve*) and regression equations reflecting selected values of P_A (*dashed curves*) are superimposed on the scatterplot for the 686 cases of the 8-population study

0.000177 Age $\times F - 2.48$ ($R^2 = 0.274$), showing the threshold for necrosis to decline from 401 μm at age 35 to 255 at age 55, a decline of 36%. $\sqrt{P_A} = 0.000181$ Age $\times F - 1.83$ ($R^2 = 0.475$).

Chromate fixation

Perifibrous lipid sequestered in the depths of nonnecrotic fibrous plaques is histochemically different from lipids of the necrotic core. Chromic acid preserves necrotic core lipids for Oil red O staining in paraffin section, and this result can be enhanced by myrcene (Fig. 4e). Deep perifibrous lipids fail to demonstrate these same behaviors (Fig. 4c). Foam cell lipids are weakly reactive (Fig. 4a) except on the margins of the necrotic core where reactivity is intense (Fig. 4e).

Stochastic properties of fibroplasia

The fibroplasia which creates the substrate for subsequent atheronecrosis is discussed in the appendix. That discussion is summarized here: The smooth muscle cells which elaborate the interstitial matrix materials are thought to be scattered at random throughout the intima of the lateral thoracic aorta during growth and maturation, generating a Poisson distribution of cells. At the completion of maturation, around age 30 to 40, the numbers of cells stabilize at an average of about 12 cells between the luminal surface and the intima-media boundary. The realms occupied by these cells have an average thickness of about 13.2 μm. After age 30 to 40, the intima continues to thicken by expansion of the sizes of the realms, and by fusion of realms into clusters through the breakdown of the boundaries between them. The clusters formed from fused realms attain average thicknesses of about 30 μm at ages 60 to 69.

Discussion

Subjects whose cause of death was related to atherosclerosis tended to have greater than usual nonnecrotic intimal thickness in the lateral thoracic aorta (Tracy et al. 1983a). The findings given in the appendix imply that this thickening was due to the expansion and fusion of smooth muscle cell realms, but not to alterations in their numbers. These results are consistent with the previous findings that atherosclerosis-related causes of death were correlated with intimal thickness but not with smooth muscle cell numbers in the aorta (Tracy and Kissling 1985b) and in the coronary arteries (Tracy et al. 1987a). Hence, the initial Poisson scatter of realms during growth and development seems to be of little consequence to clinical disease in later life. Rather, the expansion of matrix materials is the matter of greater importance. This matter has begun to receive attention recently (Ross et al. 1984). The visualization of these processes with the help of reticulin stains is described elsewhere (Tracy et al. 1987b).

The emergence of necrotic cores in the intima of the aorta and of the coronary arteries becomes more likely with age and intimal thickening (Tracy et al. 1985b; 1987a). For the thoracic aorta, that result has been reproduced here with additional cases (Fig. 3). The same results were seen with the abdominal aorta using different methodology (Fig. 2). The finding of the same results in studies of different parts of the arterial tree using various methodologies help to establish the validity of the conclusions.

These results can be rationalized in terms of the hypothesis that sequestered lipid becomes toxic with age: The noxious effect of sequestered lipid may be due to its amount, its toxicity, or both. Suppose that (F-C) is the surplus of nonnecrotic intimal thickness, F, beyond a "normal" amount, C. Also suppose that (F-C) grows in increments of size ΔF that tend to occur at equal time intervals of size α. Let φ quantify the noxious effect of sequestered lipid present in this increment. Then the total noxious effect of lipids present in (F-C) over n time periods is equal to

$$\varphi[\alpha n + \alpha(n\text{-}1) + \ldots + \alpha]. \quad (1)$$

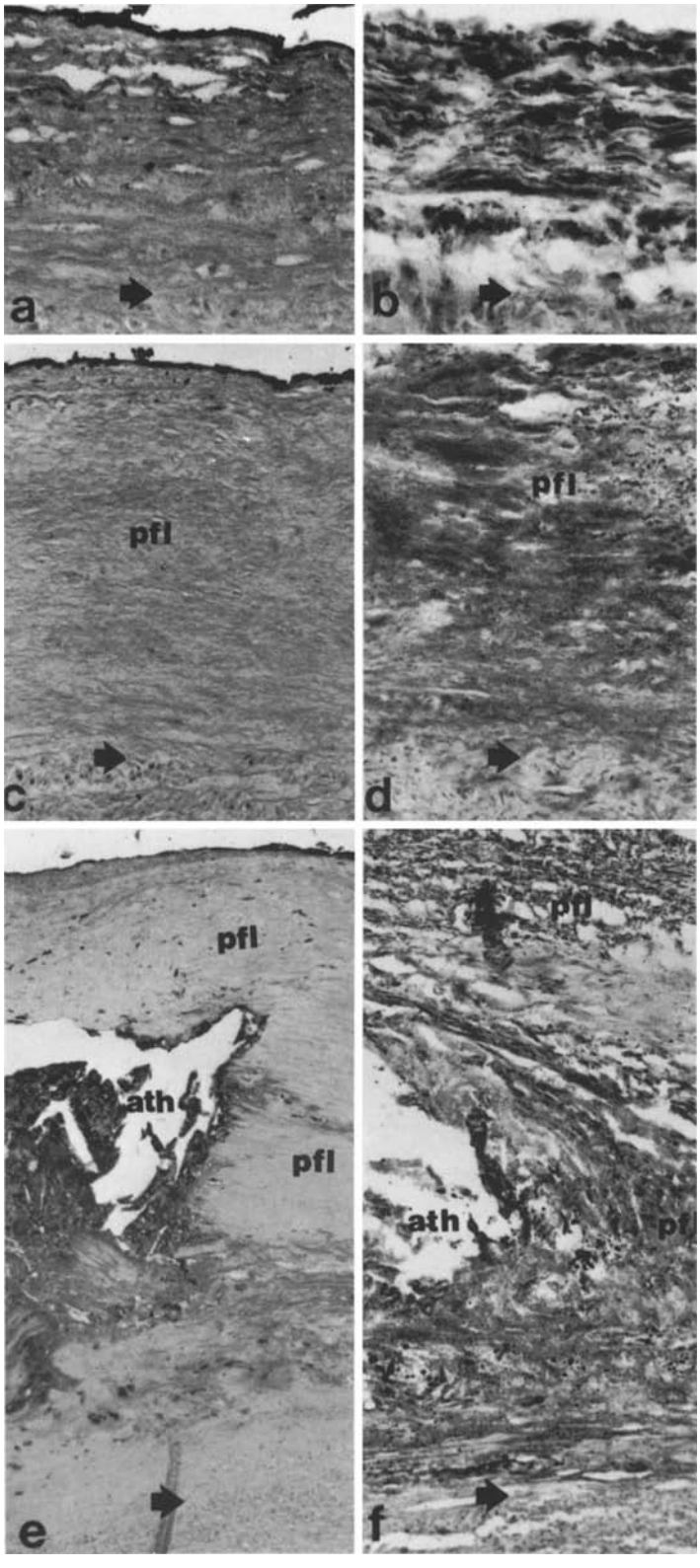

Fig. 4. Frozen (**b, d, f**) and chromate-fixed paraffin (**a, c, e**) sections of facing tissues reveal lipid of an atheronecrotic core (**e, f**), deep sequestered perifibrous lipid (**c, d**), and superficial foam cells of a fatty streak (**a, b**). ORO, ×250 (**a, b**), ×125 (**c, d**), ×60 (**e, f**)

This is the summation of all of the increments acting over the times of their existence and can be conveniently measured in units of micrometer-years. As n grows large, this sum is approximately $1/2\ n^2\ \varphi\ \alpha$ because $n+(n\text{-}1)+\ldots+1$ is $n(n+1)/2$ or approximately $1/2\ n^2$. Since $n\cdot\alpha=$Age and because $n\cdot\varphi$ is proportional to $n\cdot\Delta F=(F\text{-}C)$, the total noxious effect in equation (1) is proportional to Age $\times$ $(F\text{-}C)$, as observed repeatedly in the regression and disciminant function analyses reported here.

Figure 4 illustrates these concepts photographically. At an early stage of fibroplasia, modest amounts of young lipid are readily processed by viable foam cells (Fig. 4b). Such lipid is preserved by chromic acid in only trace amounts (Fig. 4a). Thicker intima tends to sequester more lipid (Fig. 4d). Prior to reaching the threshold for necrosis, this perifibrous lipid fails to respond to the chromation procedure (Fig. 4c). With the onset of necrosis, the debris of dead foam cells gathers along with other nondescript materials, including abundant lipid, in the necrotic core (Fig. 4f). At a necrotic focus, the core lipids can be fixed by chromic acid for staining by Oil red O in paraffin sections, while the perifibrous lipid remains unreactive (Fig. 4e). Responsiveness to chromation is, therefore, a way to demonstrate sites that are sufficiently noxious to cause massive death of incoming macrophages, and perhaps other cells as well (Gown et al. 1986).

Appendix

The lateral walls of the thoracic aorta are approximately homogeneous, so that pathological changes are scattered throughout nearly at random (Tracy et al. 1979a; 1983b; 1985a). In the first phase of atherogenesis, fibroplasia, observations can be made on the probability laws that govern the intimal growth. The building of a stochastic model begins with three empirical observations (Tracy et al. 1983b): A) In nearly every aorta, the distribution of intimal thickness over 40 nonnecrotic points was satisfactorily described by the two-parameter negative binomial distribution. B) The standard deviations of intimal thickness were better described by a quadratic function of the means of intimal thickness than by a linear relationship. C) In aortas having atheronecrosis in N of 40 points ($20<N\leqq 39$), negative binomial distributions were also adequate approximate descriptions after substitute values for the intimal thicknesses at the N censored points were estimated.

One way to derive a negative binomial distribution is to generalize a Poisson distribution by a logarithmic series distribution (Johnson and Kotz 1969). First derived by Fisher to describe the scatter of moths in a forest, this model has found wide application in biology (Fisher 1943; Quenouille 1949; Anscombe 1950; Jones and Mollison 1948). Consider, for instance, the growth of bacteria in a set of dishes. Whereas the colony counts per dish might follow a Poisson distribution with mean m_1, the numbers of bacteria per colony may have a logarithmic series distribution with parameter θ and mean $m_2=-\theta/(1\text{-}\theta)\ \log\ (1\text{-}\theta)$. Consequently, the bacterial counts per dish, X, have a negative binomial distribution with mean m_1m_2 and variance $m_1\ m_2/(1\text{-}\theta)$ (Jones and Mollison 1948). At low densities (e.g. initial plating of bacteria), X should follow a Poisson distribution with mean=

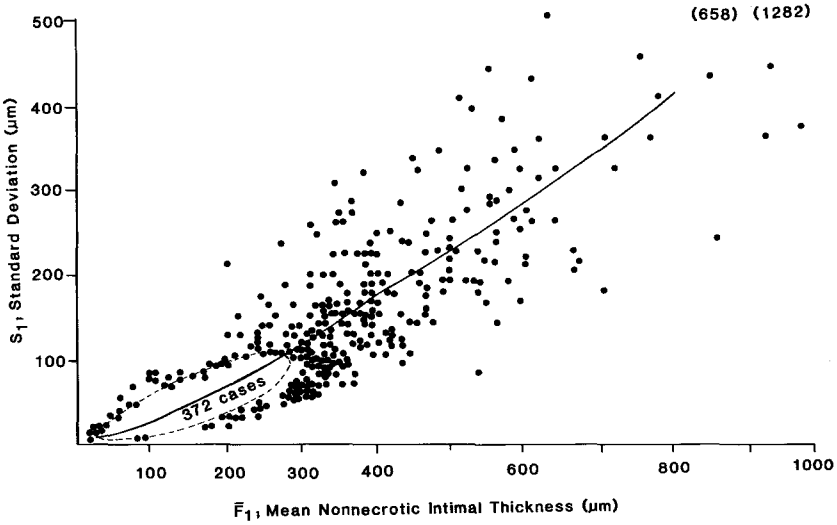

Fig. 5. Equation (1) is fitted to the scatter plot of S_1 vs. $\bar{F}_1$, with $C=40.5$, $k=13.2$ and $m_1=11.47$ (correlation coefficient = 0.866). Two off-scale points are in parentheses at the upper right. The dotted oval region is an artistic device to denote a region occupied by 372 cases so that the regression line is not obliterated by a smudge of dots

variance $= m_1$. At high densities (e.g. after the bacteria have proliferated) X should become overdispersed with variance > mean.

In the aorta, setting $X =$ the integer portion of F_1/k implies that k micrometers represents the size of an unmeasured unit, and X the number of such units. The parameters, m_1 and m_2, can be derived from the mean and variance of the negative binomial distribution of X which they determine.

$$m_1 = [(\bar{F}_1/k) \ln (S_1^2/k\bar{F}_1)]/[S_1^2/k\bar{F}_1\text{-}1] \quad \text{(A1)}$$

$$m_2 = (\bar{F}_1/k)/m_1 \quad \text{(A2)}$$

A parameter, C, emerged empirically during the curve fitting, yielding

$$m_1 = [(\bar{F}_1/k) \ln ((S_1^2\text{-}C)/k\bar{F}_1)]/[(S_1^2\text{-}C)/k\bar{F}_1\text{-}1] \quad \text{(A3)}$$

This model has 3 parameters m_1, k, and C. One of the three parameters (C) has no interpretation at this stage of model building (Logarithms are to the base e).

The mean and variance, $\bar{F}_1$ and S_1^2, are related as shown in Fig. 5. The equation, $\log (S_1^2 - 8) = 1.274 \log \bar{F}_1 - 2.66$ ($R^2 = 0.835$), was fit empirically by linear regression. Equation (A3) can also be fit to this scatter plot by nonlinear regression. Dividing through by m_1, giving unity as the dependent variable, provided estimates of $m_1 = 11.47$, $C = 40.5$, and $k = 13.2$, to minimize the sums of squares of residuals from unity ($R^2 = 0.763$). The 95% confidence intervals were $k = 9.1$ to 24.2, $m_1 = 10.99$ to 11.95, $C = 37.8$ to 43.2.

The value of k can also be estimated in another way. According to the proposed theory, the units X of width k composing the intima should follow a Poisson distribution at low cell numbers. The youngest aortas and those with the least intimal thickening should satisfy this requirement, so that setting the mean of X equal to the variance, $S_1^2/k^2 = \bar{F}_1/k$. Hence, an estimate of k is $k = S_2^2/\bar{F}_1$. In the 131 aortas with the smallest $\bar{F}_1$ (< 100 μm), the averages of $\bar{F}_1 = 70$ and of $S_1^2 = 881$, so $k = 881/70 = 12.6$. In the 30 aortas from the youngest basal subjects (age 15 to 19), average $\bar{F}_1 = 65$ and $S_1^2 = 1134$, so $k = 1134/65 = 17.4$. This approach gives 12.6 to 17.4 as reasonable values of k.

The value of $m_1 = 11.47$ represents an average over all aortas. If, however, the values of m_1 and m_2 are allowed to vary from aorta to aorta, the estimates of m_1 and m_2 can be computed for each aorta with equations (A2) and (A3) letting $k = 13.2$ and $C = 40.5$. Figure 6 shows the behavior of m_1 and m_2 in the basal and atherosclerosis cause of death groups as a function of age. The estimated m_2 tends to be weakly correlated with age in direct

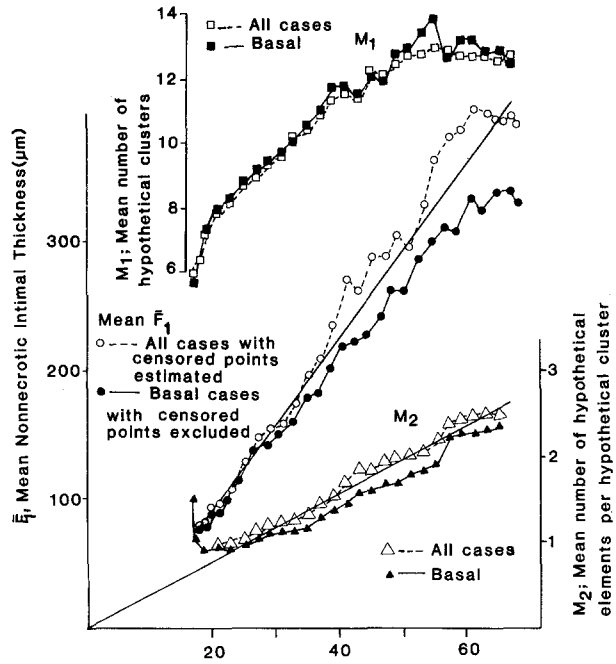

Fig. 6. Mean intimal thickness ($\bar{F}_1$) and means of hypothetical parameters m_1 and m_2 averaged aross overlapping 10-year age groups (sliding averages) are plotted for two cause of death groups. The straight line has equation $\bar{F}_1 = 6(\text{Age} - 6)$. The line through the open triangles, is $m_2 = 0.0433$ Age joining the origin to the means of all cases, $m_2 = 1.83$ at age 44.8

proportion, $m_2 = 0.0433$ Age ($R^2 = 0.056$). The behavior of m_1 as a function of age is described by $m_1 = 0.423 \text{ Age} - 0.00356 \text{ Age}^2 + 0.597$ ($R^2 = 0.148$), retaining the significant downward trend at the higher ages. Residuals from these equations are called m_{1a} and m_{2a}, and are used later in discriminant functions as age-adjusted values of m_1 and m_2.

The preceding development uses k to be the same in all aortas. Its estimated magnitude, 13.2 μm, is surprisingly close to the size of the "realm" of an average smooth muscle cell, a concept that has been elaborated elsewhere (Tracy et al. 1987b). Suppose, then, that k is allowed to vary among aortas in relation to the observed variations in the realm: If a volume of tissue, V, is found to contain C_D cells, then C_D rectangular solids with width by height by length $= K \times K \times GK = V/C_D$ would have volume V. This idealized solid figure is the realm and has size and eccentricity parameters K (width) and G (ratio of length to width) respectively. We wish to test the consequences of setting $K = k$, so that the realm is taken to be the elementary unit in our stochastic model. C_D and V have been measured in all aortas. Therefore, we could compute K if we know G.

Thomas et al. (1979) observed that the average

nuclear profile of an aortic smooth muscle cell is 19 μm long and 6 μm wide. The intima of the human thoracic aorta in youth is most commonly characterized by longitudinally oriented spindle cell nuclei. In older and thicker intima, cells tend toward a stellate shape (Orekhov et al. 1986); however, for now, assume that the typical cell is a longitudinally oriented spindle cell of unknown dimensions. A cell will be counted as present if a portion (perhaps about one-half) of its nucleus is included in either the upper or lower face of the tissue section. If, as a first approximation, the average cell has a nucleus of 6 μm diameter, and approximately one-half of this must be present to be visible, then the volume that is sampled by an 11 μm section is $(6/2+6/2+11)\times 100\times 100\ \mu m^3$. Consider the "realm" of an average cell to be shaped like its nucleus, with a length that is G times its width, K. Hence the width of one realm is $K=\sqrt[3]{(170000/G\times C_D)}$.

The actual values of G are unknown; therefore, several values were investigated, covering the range of reasonable magnitudes. From the figures of Thomas et al. (1979) the value, $G=19/6=3.17$, was given priority. Orekhov et al. (1986) isolated smooth muscle cells from formalin-fixed intima with alkaline alcohol. Photographs in their paper show spindle cells with $G=6$ to 36, averaging about 20. The values of $G=3.17$, 6, and 12 span the range that was necessary to fit the proposed model to most aortas. The value of $G=6$ was found to be generally most useful, as explained in the discussion of Fig. 7. Hence, $K=\sqrt[3]{(28333/C_D)}$ is adopted for the construction of Fig. 7 and Table 2.

In the expression, $X=\bar{F}_1/k$, substitution of $k=K=\sqrt[3]{(28333/C_D)}$ allows computation of X, the number of hypothetical units, at each of the 40 observed positions in each aorta. The frequency distributions of the 40 observations of X in each specimen can then be compared to fitted Poisson and negative binomial distributions, by Chi Square goodness of fit tests as described elsewhere (Tracy et al. 1983b). In aortas with N positions censored by atheronecrosis, 40-N observations of X at non-necrotic positions were used for curve fitting.

Arbitrarily using the value of $G=6$, the distributions of X in 100 of the 139 aortas having no atheronecrosis (No-A) were successfully fitted by a Poisson distribution, using the Chi-square goodness of fit test. These 100 aortas are plotted as closed circles in the lower of Fig. 7, a plot of the mean vs. the variance of X. Ten additional aortas could be described by Poisson distributions using $G=12$. These 10 aortas, depicted in Fig. 7 by

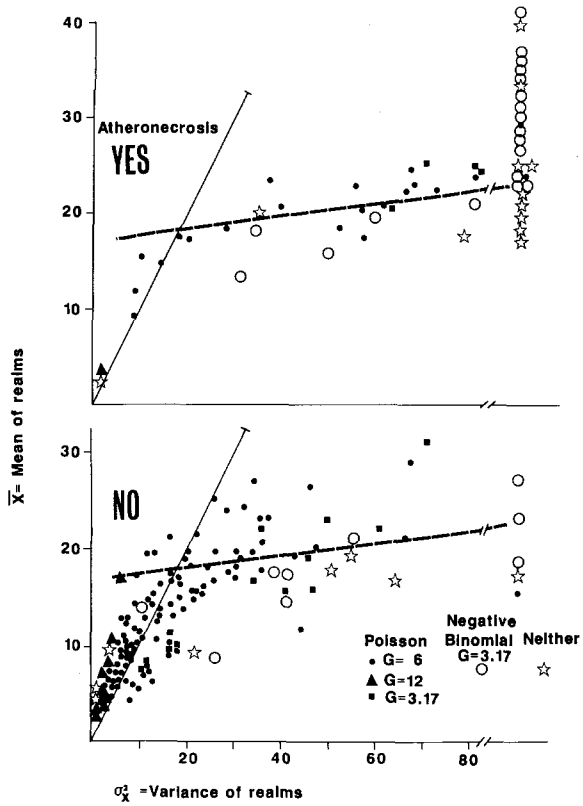

Fig. 7. The numbers of realms (X) of size k (inversely proportional to the cube root of cell density) had mean, $\bar{X}$, and variance, σ_x^2, as plotted here for 139 No-A and 57 Yes-A lateral thoracic aortas. Chi Square tests of goodness-of-fit of Poisson and negative binomial distributions were done with different values of G. G is the proportionality constant describing the ratio of the realm's length to its width. The solid line had equation $\bar{X}=\sigma_x^2$, and the dashed line, $16\bar{X}+17=\sigma_x^2$, these are reference lines introduced to aid comparison between Yes-A and No-A cases

closed triangles, had the variance much smaller than the mean when $G=6$ (left margin of the No-A plot). With $G=12$, this underdispersed condition was corrected and a Poisson distribution fitted adequately. Eight of these 10 cases were of age 15 to 35, and all of them had intimal thickness less than 130 μm. Another 12 aortas could be described by Poisson distributions using $G=3.17$. These 12 aortas, represented by squares in Fig. 7, had the variance greatly in excess of the mean when $G=6$ (lower-right margin of the No-A scatter of points). By use of $G=3.17$, this overdispersed condition was corrected and a Poisson distribution fitted adequately. Seven of these 12 cases were of age 35 to 65 and 8 of them had intimal thickness of 130 μm to 415 μm. Nine other No-A aortas (open circles in Fig. 7) could not be described by the Poisson distribution using any of these choices of G, and were successfully fitted to the negative binomial.

Table 2. Mean number of smooth muscle cells, mean nonnecrotic intimal thickness, variance of the nonnecrotic intimal thickness, size of an average smooth muscle cell realm, parameters m_1 and m_2 of the negative binomial process model and numbers of aortas by age group for two cause of death groups

	Age Group					
	15–19	20–29	30–39	40–49	50–59	60–69
Basal causes of death						
$\bar{C}_T$ (Cells); units	13.2	18.6	22.8	27.9	25.7	22.0
$\bar{F}_1$ (Thickness); μm	65	112	164	227	292	333
S^2 (Variance of $\bar{F}_1$); μm^2	1134	2277	4980	12366	20283	38272
k_r (Size of realm); μm	11.3	11.6	12.1	12.8	14.2	15.7
m_1 (Clusters); units	5.9	9.1	10.8	12.3	13.6	12.1
m_2 (Units per cluster)	1.07	1.10	1.24	1.57	1.79	2.11
N (Cases)	30	95	86	71	73	100
Athero-related causes of death						
$\bar{C}_T$ (Cells); units	17.8	24.4	24.7	28.9	27.6	21.4
$\bar{F}_1$ (Thickness); μm	122	164	226	330	378	407
S^2 (Variance of $\bar{F}_1$); μm^2	2361	5481	19779	31322	44222	39339
k_r (Size of realm); μm	11.7	11.8	13.0	14.3	14.9	17.3
m_1 (Clusters); units	8.4	10.3	11.4	12.8	11.8	11.7
m_2 (Units per cluster)	1.08	1.47	2.21	2.49	2.49	2.29
N (Cases)	4	17	25	33	40	74

k_r is the mean size of realm, k, using $G=6$ in the expression $k=\sqrt[3]{(170000/GC_D)}$

Having confirmed some theoretical predictions with observational data, it becomes necessary to also inquire whether the parameters of the model aid in understanding clinically important disease. For this purpose, two cause of death groups were compared: atherosclerosis-related vs. basal. With k fixed at 13.2 μm for all aortas, the parameters m_1 and m_2 can be derived from equations (2) and (3). The mean number of hypothetical units per cluster (m_2) was larger in atherosclerosis related cause of death cases than in basal cases at all ages (Fig. 6). The mean number of clusters (m_1) per aorta did not differ between the two cause of death groups (Fig. 6). This matter was also examined by linear discriminant functions. After age adjusting m_1 and m_2 with polynomial regression equations to give the age adjusted values, m_{1a} and m_{2a}, the discriminant function $D=0.558\ m_{1a}+1.137\ m_{2a}$ was obtained for distinguishing the 474 basal from the 212 atherosclerosis-related (standardized coefficients, significant at $\alpha=0.05$ and $R^2=0.0552$). This low R^2 reflects the fact that the measurements made in the thoracic aorta are of limited value for distinguishing cases by cause of death. However, these results suggest that both m_1 and m_2 are of some additive significance and that m_2 is about twice as important as m_1 in distinguishing cause of death groups.

Allowing k to vary among aortas according to $k=\sqrt[3]{(170000/GC_D)}$, and using $G=6$, m_1 and m_2 can be obtained from equations (1) and (2). Again m_2 was larger in atherosclerosis-related than basal groups at all ages (Table 2). The estimates of k were also larger in atherosclerosis-related than basal groups at all ages. Again, the mean number of clusters, m_1, differed little between the two cause of death groups, and the differences were inconsistent among the age groups. A discriminant function distinguishing the two cause of death groups yielded $D=0.243\ m_{2a}+0.399k_a$ (standardized coefficients, m_{2a} and k_a are age adjusted by cubic regression equations, $R^2=0.0511$). The function did not accept m_{1a} as significant. These results identify the width of the realm of an average smooth muscle cell, and the average number of such realms per cluster as the most important variables to distinguish the two cause of death groups. The number of realms, which reflects the number of cells, was of relatively little importance.

Acknowledgements. This work was supported by Grant No. HL08974 entitled "Natural and Experimental Atherosclerosis". Manuscript by Monique Ardoin; Photos by Gene Wolfe.

References

1. Anscombe FJ (1950) Sampling theory of the negative binomial and logarithmic series distributions. Biometrika 37:358–382
2. Benditt EP (1977) The origin of atherosclerosis. Sci Am 236:74–85
3. Chait A (1983) The role of lipoprotein receptors in lipid transport and in the pathogenesis of the hyperlipoproteinemias. Special Topics Endocrin Metabol 5:1–53

4. Ferrario JB, DeLeon IR, Tracy RE (1985) Evidence for toxic anthropogenic chemicals in human thombogenic coronary plaques. Arch Environ Contamin Toxicol 14:529–534
5. Fisher RA (1943) Species and the Number of Individuals in a Random Sample of an Animal Population. J Animol Ecology 12:42–57
6. Gown AM, Tsukada T, Ross R (1986) Human Atherosclerosis. II Immunocytochemical Analysis of the cellular composition of human atherosclerotic lesions. Am J Pathol 125:191–207
7. Jachau MR, Bond JA, Kocan RM, Benditt ER (1970) Bioactivation of polycyclic aromatic hydrocarbons in the aorta: Evidence for a role in the genesis of atherosclerotic lesions. In: Jones PW, Leber P (eds) *Polycyclic Aromatic Hydrocarbons*. Ann Arbor Science Publishers, Ann Arbor, MI, pp 639–652
8. Johnson NL, Kotz S (1969) *Discrete Distributions*. John Wiley, New York
9. Jones PCT, Mollison JE (1948) A technique for the estimation of soil micro-organisms. J General Microbiology 2:54–69
10. Kritchevsky D, Tepper SA, Kim HK, Story JA, Vesselinovitch D, Wissler RW (1976) Experimental atherosclerosis in rabbit fed cholesterol-free diets 5. Comparison of peanut, corn, butter and coconut oils. Exp Mol Pathol 24:375–391
11. Malcom GT, Strong JP, Restrepo C (1984) Atherosclerosis and lipid composition of the abdominal aorta. Lab Invest 50:79–86
12. Orekhov AN, Kalantarov GF, Andreeva ER, Prokazova NV, Trakht IN, Bergelson LD, Smirnov VN (1986) Monoclonal antibody reveals heterogeneity in human aortic intima: Detection of a ganglioside antigen associated with a subpopulation of intimal cells. Am J Pathol 122:379–385
13. Quenouille MH (1949) A Relation between the Logarithmic, Poisson and Negative binomial series. Biometrics 5:162–164
14. Ross R, Wight TN, Strandness E, Thiele B (1984) Human Atherosclerosis. I. Cell constituents and characteristics of advanced lesions of the superficial femoral artery. Am J Pathol 114:79–93
15. Scott RF, Morrison ES, Jarmolych J, Nam SC, Kroms M, Coulston F (1967) Experimental atherosclerosis in rhesus monkeys. I. Gross and light microscopy features and lipid values in serum and aorta. Exp Mol Pathol 7:11–33
16. Smith EB, Ashall C (1984) Compartmentalization of water in human atherosclerotic lesions. Arteriosclerosis 4:21–27
17. Stary HC (1984) Location and development of atherosclerotic lesions in coronary arteries. Atherosclerosis 50:237–239
18. Taylor CB, Peng SK, Werthesen NR, Tham P, Lee DT (1979) Spontaneously occurring angiotoxic derivatives of cholesterol. Am J Clin Nutr 32:40–57
19. Thomas WA, Reiner JM, Florentin RA, Scott RF (1979) Population dynamics of arterial cells during atherogenesis VIII. Separation of the roles of injury and growth stimulation in early aortic atherogenesis in swine originating in pre-existing intimal smooth muscle cell masses. Exp Mol Pathol 31:124–144
20. Tracy RE, Strong JP, Toca VT, Lopez CR (1979a). Variable Patterns of Nonatheromatous Aortic Intimal Thickening. Lab Invest 41:553–559
21. Tracy RE, Strong JP, Toca VT, Lopez CR (1979b) Atheronecrosis and Its Fibroproliferative Base and Cap in the Thoracic Aorta. Lab Invest 41:546–552
22. Tracy RE, Toca VT, Lopez CR, Kissling GE, Devaney K (1983a) Fibrous intimal thickening and atheronecrosis of the thoracic aorta in coronary heart disease. Lab Invest 48:303–312
23. Tracy RE, Toca VT, Kissling GE, Lopez CR (1983b) Fibrous Intimal Thickening Atheronecrosis of the Thoracic Aorta: Some Background for Mathematical Theory. Lab Invest 48(3):313–322
24. Tracy RE, Kissling GE, Devaney DO, Lopez CR, Gardia M (1985a) Spatial dispersion of spindle cells in the human thoracic aorta. Lab Invest 52:85–92
25. Tracy RE, Kissling GE (1985b) Age and Fibroplasia as preconditions for atheronecrosis in the human thoracic aorta. Arch Pathol Lab Med 109:651–658
26. Tracy RE, Kissling GE, Lopez CR, Gandia M (1986). Morphometric features of atherosclerosis which vary or remain constant in 8 populations. Lab Invest 54:314–321
27. Tracy RE, Kissling GE (1987a) Age and fibroplasia as preconditions for atheronecrosis in human coronary arteries. Arch Pathol Lab Med (In press)
28. Tracy RE, Kissling GE, Curtis MB (1987b) Smooth muscle cell-reticulin lamellar units of 13.2 μm thickness composing the aortic intima. Virchow Arch A 411:415–424
29. Van Lier JE, Smith LL (1967) Sterol metabolism. I 26-hydroxycholesterol in the human aorta. Biochemistry 6:3269–3278
30. Velican C, Velican D (1985) Study of coronary intimal thickening. Atherosclerosis 56:331–344
31. Wigglesworth VB (1981) The distribution of lipid in the cell structure. Tissue Cell 13:19–34
32. Wissler RW (1974) Atherosclerosis – its pathogenesis in perspective. Adv Cardiol 13:10–33

Accepted June 1, 1987